Acta Montanistica Slovaca
ISSN 1335-1788
actamont.tuke.sk

Leveraging Artificial Neural Networks to Predict Igneous Rock Strength Parameters from Petrological Contents

Javid HUSSAIN[1,2,3,4], Nafees ALI[1,2,3,4], Xiaodong FU[1,2,3,4], Jian CHEN[1,2,3,4], Naveed Ahmed KHAN[5] and Sartaj HUSSAIN[1,2]*

Authors' affiliations and addresses:
[1] State Key Laboratory of Geomechanics and Geotechnical Engineering, Institute of Rock and Soil Mechanics, Chinese Academy of Sciences, Wuhan 430071
Country: China

[2] University of Chinese Academy of Sciences, Beijing 100049, China

[3] China-Pakistan Joint Research Center on Earth Sciences, Islamabad 45320, Pakistan

[4] Hubei Key Laboratory of Geo-Environmental Engineering, Wuhan 430071, China

[5] Chinese Academy of Sciences, Beijing

***Correspondence:**
Jian Chen, State Key Laboratory of Geomechanics and Geotechnical Engineering, Institute of Rock and Soil Mechanics, Chinese Academy of Sciences, Wuhan 430071
tel.:15623001580
e-mail: jchen@whrsm.ac.cn

Acknowledgement:
We would like to express our sincere gratitude to everyone who contributed, both directly and indirectly, throughout this research. Additionally, we extend our heartfelt thanks to the ANSO Scholarship for Young Talents Program for supporting our research at the University of the Chinese Academy of Sciences (UCAS), China. Javid Hussain is an awardee of the ANSO Scholarship 2023-PhD.

How to cite this article:
Hussain, J, Ali, N., Fu, X., Chen, J., Khan, N.A. and Hussain, S. (2025) Leveraging Artificial Neural Networks to Predict Igneous Rock Strength Parameters from Petrological Contents. *Acta Montanistica Slovaca,* Volume 30 (2), 470-491

DOI:
https://doi.org/10.46544/AMS.v30i2.16

Abstract
Accurately determining rock strength characteristics, such as uniaxial compressive strength (UCS), Brazilian tensile strength (BTS), and Los Angeles Abrasion (LAA), through conventional methods is both time-consuming and resource-intensive. To address this challenge, this study develops efficient artificial neural network (ANN) models optimized with Levenberg-Marquardt (LM), Bayesian Regularization (BR), and Scaled Conjugate Gradient (SCG) algorithms to predict UCS, BTS, and LAA from petrographic properties, advancing civil engineering applications. A total of 100 dolerite samples were analyzed to assess their strength and petrographic characteristics, with the ANNs trained on the three aforementioned algorithms. The results indicate that the BR model achieved the highest accuracy, with a correlation coefficient (R) of 0.9999 and a root mean square error (RMSE) of 0.3164. The LM model also demonstrated strong performance with an R-value of 0.9997 and an RMSE of 0.8619. The BR and LM models significantly outperformed the SCG model, which had an R-value of 0.9954 and an RMSE of 2.398. Sensitivity analysis identified plagioclase and chlorite as the most influential factors in predicting rock mechanical parameters. The effectiveness of the BR and LM techniques highlights their potential to offer substantial time and cost savings in rock strength prediction.

Keywords
Engineering Properties; Petrographic analyses; Predictive Relationships; ANNs; Sensitivity Analyses

1. Introduction

The mechanical properties of intact rocks are significantly influenced by their mineralogical and textural characteristics. Therefore, a thorough understanding of these attributes is essential for accurately assessing and predicting the mechanical behaviours of rocks. Various mineralogical and textural elements play crucial roles in shaping a rock's mechanical properties, including its mineral composition, density, hardness, size, shape, degree of interlocking, type of grain contacts, packing density, quantity, and the nature of cement and matrix. In the laboratory setting, these attributes can be efficiently and effectively evaluated through standard thin-section analyses, providing valuable insights into rocks' internal structure and composition (Khajevand and Fereidooni, 2018).

Assessing the mechanical qualities of the material (rock and soil) is essential before developing a specific engineering project (Hussain et al., 2023; Hussain et al., 2024). However, several tests are carried out in the laboratory to assess the strength and deformation properties of rock, such as the Brazilian tensile strength (BTS) test, the unconfined compression strength (UCS) test and the Los Angles abrasion test (LAA), which have been standardized by the American Society for Testing and Materials (ASTM) and the International Society for Rock Mechanics (ISRM). The unconfined axial compression is a laboratory test that directly measures the UCS, BTS, and LAA of rock samples. Nevertheless, certain obstacles exist to directly assessing the aforementioned rock properties in the laboratory. Obtaining sufficient high-quality core samples can be challenging, particularly in rocks that are extensively fractured, weak, and fragmented (Momeni et al., 2015; Stroisz et al., 2025). In addition, these direct technique tests include numerous disadvantages that are time-consuming and costly (Jahed Armaghani et al., 2016).

The use of indirect tests, such as Petrographic characteristics, for their prediction is more advantageous and suitable since they are less expensive and simpler to carry out than the traditional UCS, BTS, and LAA test techniques, which need expensive equipment (Hussain et al., 2024). The majority of scholars attempted to use the ANNs technique to examine the strength parameters of rock indirectly due to the disadvantages of determining UCS directly. Through thin-section analysis, Saffet Yagiz investigated and evaluated the physicochemical properties of the rocks in the laboratory. To quantify important rock qualities and VP, he came up with several empirical equations, which he then used for the statistical analysis to confirm. He discovered a relationship between rocks' engineering (shear strength) properties and the composition of their surfaces and mineral particles. So, the best VP correlation coefficient between UCS and E was achieved, coming in at 0.94 (94% confidence level) and 0.91 (91% confidence level) (Yagiz, 2011).

Furthermore, many researchers have examined the relationship between mineralogical and textural features and mechanical characteristics of different rocks (Hussain et al., 2025). They have discovered significant relationships between these parameters, highlighting the crucial role of these components in determining the mechanical behaviours of rocks. The researcher analyzed the petrographic characteristics and engineering geological parameters, such as modulus ratio, elastic constant ratio, triaxial compressive strength (TCS), and UCS, to categorize the carbonate hard ground (Dogan et al., 2006). The UCS and elastic modulus (E) of a fault breccia from the texture coefficient (TC) were predicted by using regression analysis, and they concluded that the UCS of the tested breccia is highly associated with TC (Alber and Kahraman, 2009).

Furthermore, the prediction of the UCS based on textural abilities was carried out through an artificial neural network and multivariate regression(Manouchehrian, Sharifzadeh and Moghadam, 2012). Moreover, previous researchers employed regression analyses to predict the engineering properties of limestone and marble samples based on microscopic data by regression analyses(Ozcelik, Bayram and Yasitli, 2013). The effects of texture and mineralogy were determined by using the ANN approach on the mechanical behaviour of marble samples (Bandini and Berry, 2013). Additionally, Kamani (Kamani and Ajalloeian, 2019) assessed the engineering characteristics of carbonate rocks using the adjusted texture coefficient and found that this metric can accurately evaluate and categorize the engineering characteristics of carbonate rocks in real-world scenarios. Researchers used image-based textural quantification techniques to analyze crystalline igneous rocks and how their mineralogy and textural properties affect their strength (Hemmati et al., 2020). They stated that their developed indicator for quartz to feldspar size ratio was a highly effective texture measure. This parameter is strongly correlated with compressive and tensile strength across various rock types.

While previous research has focused extensively on predicting the mechanical properties of rocks, particularly Uniaxial Compressive Strength (UCS), by analyzing their mineralogical and textural characteristics, there remains a significant gap in comparative studies that assess the effectiveness of various predictive models for these properties. Most existing studies have relied on traditional empirical methods or individual algorithms without exploring or comparing multiple advanced models. Furthermore, few studies have integrated comprehensive petrographic attributes as input variables to simultaneously predict multiple mechanical strength parameters. This study addresses these gaps by examining 100 Dolerite rock samples to analyze their petrographic, textural, and mechanical properties. The research specifically aims to develop and compare three different Artificial Neural Network (ANN) models, BR, SCG, and LM, for predicting key mechanical strength parameters: UCS, Brazilian

Tensile Strength (BTS), and Los Angeles Abrasion (LAA). While ANN techniques have been used in some studies, the comparative analysis of these three models for predicting rock strength has not been fully explored in the existing literature (López, 2023).

The novelty of this research lies in its approach to directly comparing the performance of BR, SCG, and LM models, incorporating a variety of petrographic attributes as inputs and assessing their accuracy in predicting UCS, BTS, and LAA. The optimal model selection is based on two critical statistical indicators: the correlation coefficient (R-value) and the mean square error (MSE). A Taylor diagram is used for a visual comparison of model performances. Additionally, a sensitivity analysis is conducted to evaluate the influence of each input variable on the mechanical strength parameters. By addressing the lack of comparative analysis in ANN-based predictive modelling for rock strength, this study comprehensively evaluates how different models perform with varied input data and mechanical outputs. This research fills the gap in the literature by offering a more nuanced understanding of model effectiveness, making it a valuable contribution to both geological research and engineering applications.

2. Materials and Methods

The present study involved fieldwork and laboratory analyses conducted in the Kirana Hills region to investigate the geotechnical and petrographic properties of Dolerite aggregates.

Furthermore, Artificial Neural Networks (ANN) were employed to predict UCS, BTS, and LAA based on mineral composition and textural properties of Dolerites. The LM, BR, and SCG learning approach was utilized to train an ANN using a dataset of 100 detrital rock samples, as shown in Figure 1. The mineralogical composition of these rock samples also encompassed information about the composition through petrographic analyses.

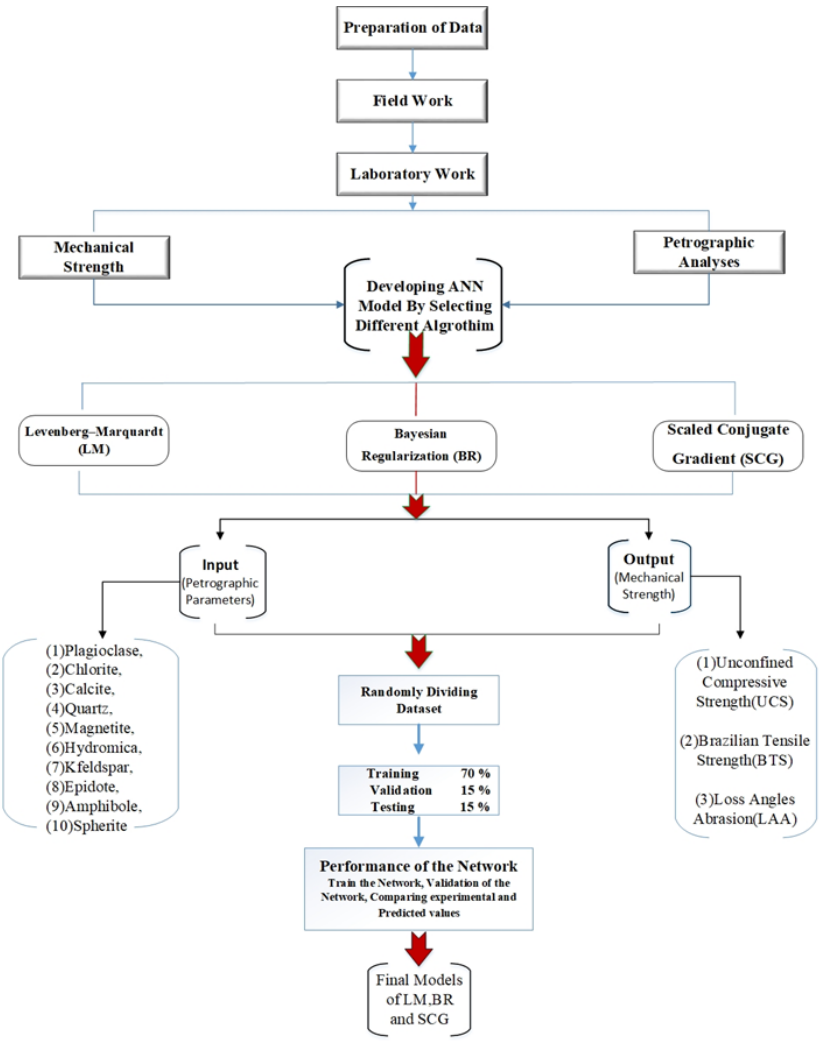

Fig. 1. *Flow chart of the research work*

2.1 Geological setting of the collected samples

The Kirana-Malani Basin, also known as the Punjab Foreland Basin, originated in the Late Proterozoic era within the Northeast Gondwana region of Greater India (Khan et al., 2017). It is characterized by the prevalence of rhyolitic masses and some dolerite/basalt, andesite, and dacite outcrops, as shown in Figure 2. The Kirana Hills, situated near Sargodha, Chiniot, Shah Kot, and Sangla Hills, consist predominantly of Proterozoic rocks devoid of Phanerozoic lithologies(Hussain et al., 2022). The Kirana Hill rocks are considered the underlying basement for the sedimentary cover sequence, ranging from Paleozoic to Cambrian. These rocks in the Kirana Hills hold significant economic value as they are a crucial source of aggregates for constructing roads and civil structures in the Punjab province of Pakistan.

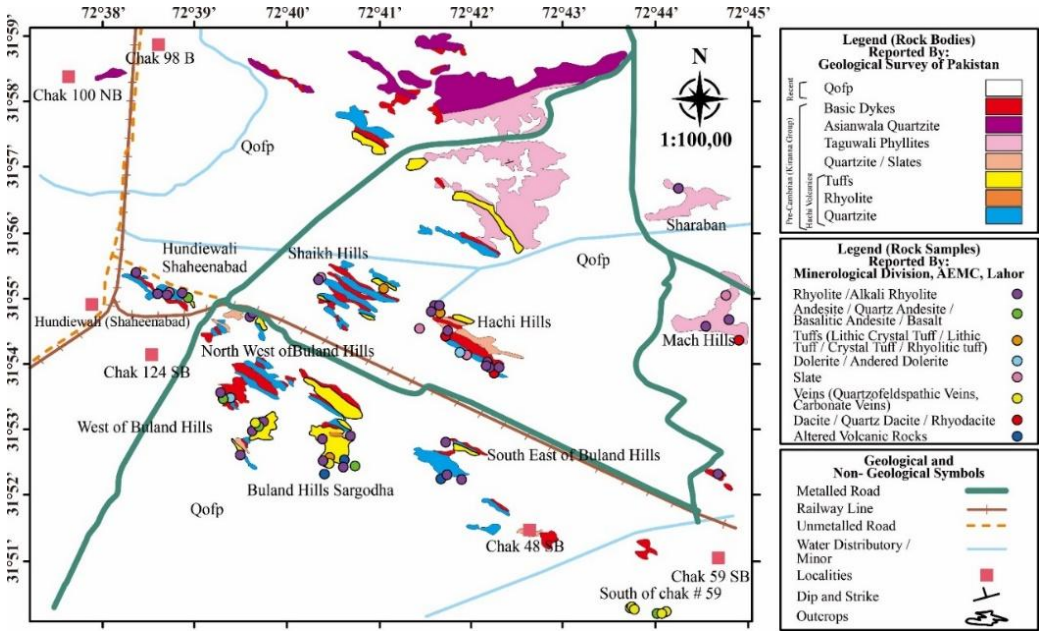

Fig. 2. *The Geological Map of Kirana Hills, Pakistan, shows the spatial distribution of various rock types and geological formations in the Kirana Hills region. The map includes detailed legends that differentiate rock bodies and samples based on their mineralogical and geological characteristics. Additionally, the map shows important geographic coordinates, town names, and the scale bar (1:100,000) for reference. Geological boundaries, such as those of the Buland Hills and the surrounding areas, are outlined, providing a comprehensive view of the area's geologic composition.*

2.2 Petrographic Analyses

Petrographic investigations are performed to establish the depositional and chemical positions of the rock comprising the aggregate and its mineralogy. Petrographic assessments are often used to detect the reactive constituents in aggregates (Ugur, Demirdag and Yavuz, 2010). The comprehensive petrographic investigation aims to determine the influence of probable depositional environments and diagenetic fabric on the engineering qualities of the understudied rocks. The mineral content was determined via a model analysis approach. The proportion of minerals was calculated using Equation 1.

$$C_m = (T_m / T_{tm}) * 100 \qquad (1)$$

Where C_m is the % of mineral composition, T_m is the Total number of counts for a mineral, and T_{tm} is the Total number of counts for the entire mineral.

2.3 Geotechnical Analyses

The research conducted an in-depth assessment of the characteristics of mechanical strength. The rock strength parameters examination included UCS, BTS, and LAA tests.

2.3 Geotechnical Analyses

2.3.1 Unconfined Compressive Strength (UCS)

UCS enumerates the maximum axial stress that rock can endure before fracturing. Rock strength is often evaluated by laboratory testing to determine its ability to withstand stress, enabling the identification of a suitable rock for a certain purpose(Deere and Miller, 1966). The UCS was calculated according to the (C170-17, 2017) by using equation 2.

$$\sigma_c = F/A \quad (2)$$

In which σ_c is the uniaxial compressive strength (MPa), F is the maximum failure load (in N), and A is the cross-sectional area (mm^2).

2.3.2 Brazilian Tensile Strength (BTS)

In natural conditions, rock masses are typically subjected to compression rather than tension directly. However, tension can occur indirectly through the transfer of compression. Conducting direct tensile strength tests on rocks is challenging and often expensive for routine applications(Woodland et al., 2023). As an alternative, the Brazilian disk test is commonly used to define rock samples' tensile strength. This test maintains the thickness-to-diameter ratio at 1:2. The BTS test was calculated using equation 3.

$$\sigma_t = 2P/\pi\, d\, t \quad (3)$$

In which σ_t is the tensile strength (MPa), P is the failure load (N), d is the diameter of the specimen (mm), and t is the thickness of the specimen (mm).

2.3.3 Los Angles Abrasion (LAA)

The LAA test was conducted according to ASTM C131/C131M (2014) guidelines (ASTM, 2008). For each LAA test, 5000 ± 10 g of the graded aggregate sample and 12 steel spheres were employed in the Los Angeles machine cylinder. The cylinder was rotated 500 times, and the Percentage of fines passing through the 1.70 mm sieve was measured. Equation 4 was used to calculate the LAA %.

$$LAA_{losses}\,(\%) = A - B/(1) * A * 100 \quad (4)$$

where A is the original mass of samples(g), and B is the final mass of samples retained on the number 12 sieve in grams.

2.4 Artificial Neural Network (ANN)

Artificial Neural Networks (ANN) have recently been utilized in various geotechnical models. Numerous studies suggest that machine-learning approaches are more efficient and effective than traditional methods (Pianosi et al., 2016). Neural networks acquire knowledge by processing the provided instances rather than relying on pre-established mathematical relationships between variables (Borgonovo and Plischke, 2016). Neural networks are often trained by processing large input and output patterns to achieve pattern recognition and prediction. The technique involves establishing a connection between input and output data. Consequently, it has remarkable interpolation abilities, particularly when the input data is contaminated by noise. Neural networks may replace statistical analysis approaches such as auto-correlation, multivariable regression, linear regression, trigonometric functions, etc. Three fundamental components could define a particular network: transfer function, network architecture, and learning legislation(Khan et al., 2021). The choice of these components will fluctuate depending on the problem to be resolved. Figure 3 shows the general framework of the ANN.

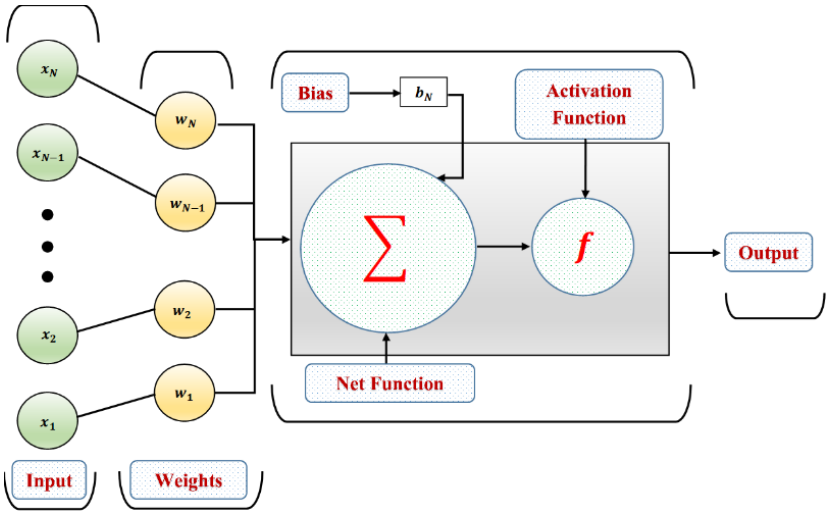

Fig. 3. *General Architecture of ANN*

2.4.1 Dataset

In this study, three artificial neural network (ANN) algorithms, Bayesian Regularization (BR), Scaled Conjugate Gradient (SCG), and Levenberg-Marquardt (LM), were selected to predict key mechanical strength parameters (UCS, BTS, and LAA) based on petrographic data. These algorithms were chosen for their distinct characteristics and suitability to the problem at hand. The Levenberg-Marquardt (LM) algorithm was selected due to its fast convergence properties and high accuracy in solving non-linear problems, particularly when dealing with relatively small datasets, which is a common scenario in geotechnical engineering studies. It has proven highly effective in similar applications where complex relationships must be captured efficiently. The Bayesian Regularization (BR) algorithm was chosen for its ability to mitigate overfitting and its robustness in handling noisy data, making it particularly valuable when the dataset is limited or contains variability, as is often the case in rock strength prediction. BR enhances model generalization, ensuring reliable predictions even with complex input-output relationships. The Scaled Conjugate Gradient (SCG) algorithm, although less computationally efficient, was included for comparative analysis. SCG has been successfully applied in geotechnical modelling and was assessed to provide a baseline for evaluating the performance of LM and BR. By utilizing these three algorithms, we aimed to explore their respective strengths and limitations in rock strength prediction, thereby contributing to a comprehensive evaluation of ANN-based models in geotechnical applications. The architecture of the neural network is based on a dataset obtained from petrographic and geotechnical analyses. This dataset is split into two parts: input data and target data. The input data comprises the features fed into the neural network, while the target data represents the expected outcomes for each corresponding input. The dataset is fundamental in shaping the network's design, influencing factors such as the number and types of layers, as well as defining its parameters (Khan *et al.*, 2022). The network consists of three distinct phases: training, validation, and testing. Table 1 displays the data division for the model's training, validation, and testing.

Tab. 1. *Data Splitting for model, testing, training, and validation*

Levenberg-Marquardt Algorithm(LM)		
Phase	Percentage (%)	No of Specimens
Training	70	70
Validation	15	15
Testing	15	15
Total	100	100
Bayesian Regularization (BR)		
Training	75	75
Validation	-	-
Testing	25	25
Total	100	100
Scaled Conjugate Gradient (SCG)		

Training	70	70
Validation	15	15
Testing	15	15
Total	100	100

This research used a neural network model with 10 input parameters and three output parameters to predict the strength characteristics of materials and evaluate knowledge regarding rock types. The input parameters correspond to the following rock types: sphalerite, hydromica, chlorite, quartz, calcite, hydromica, epidote, amphibole, and feldspar, as seen in Figure 4. The neural network processes this information by assigning numerical codes to categorize each kind of rock. The output parameters give precedence to crucial mechanical strength properties, including UCS, BTS, and LAA. These qualities are determined using laboratory experiments following the prescribed methodologies established by the International Society for Rock Mechanics (ISRM) (Culshaw, 2015).

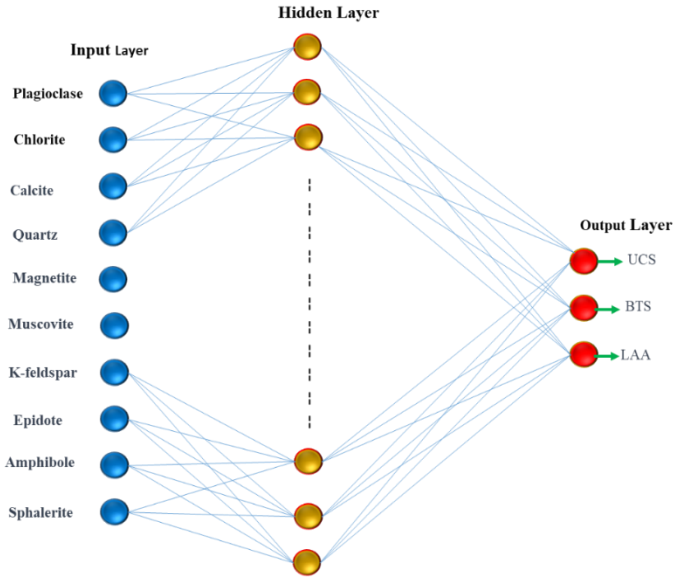

Fig. 4. *Architecture of Input and Output*

2.4.2 Statistical Analysis between Variables

The heatmap in Figure 6 was utilized to calculate the correlation coefficients among various parameters. The analysis reveals intricate relationships between these parameters, offering insight into how mineralogical factors influence the mechanical properties of rocks. The heatmap visualizes the strength and direction of correlations between variables, with values ranging from -1 to 1, where values closer to 1 indicate a strong positive correlation, values closer to -1 indicate a strong negative correlation, and values near 0 suggest weak or no correlation. From the heatmap, it is particularly noteworthy that Calcite (Calc) shows a strong positive correlation with several mechanical strength parameters, including UCS, BTS, and LAA, with Pearson correlation values of 0.3172, -0.4030, and 0.2501, respectively, as shown in Figure 5. This suggests that Calcite has a considerable impact on the rock's mechanical properties, particularly in relation to its compressive strength (UCS) and abrasion resistance (LAA). Additionally, Micrite (Mic) and Spherite (Sph) also exhibit positive correlations with UCS, BTS, and LAA, further emphasizing the significant role of these mineralogical components in affecting the mechanical strength of the rock. Notably, Plagioclase (Pl) and Chlorite (Chl) show weaker correlations with the mechanical properties, as indicated by their relatively lower Pearson correlation values. This suggests that while they play a role in influencing rock strength, their impact is not as pronounced as that of Calcite, Micrite, and Spherite.

The results from the heatmap suggest a compelling relationship between the composition of these minerals and the mechanical properties being studied. The strong correlations observed between certain minerals (e.g., Calcite and UCS, BTS, and LAA) underscore the complexity and depth of the underlying geological dynamics that influence rock behaviour. These findings provide valuable insights into how mineral composition impacts the mechanical strength of rocks, which is crucial for geotechnical applications such as material selection and engineering design.

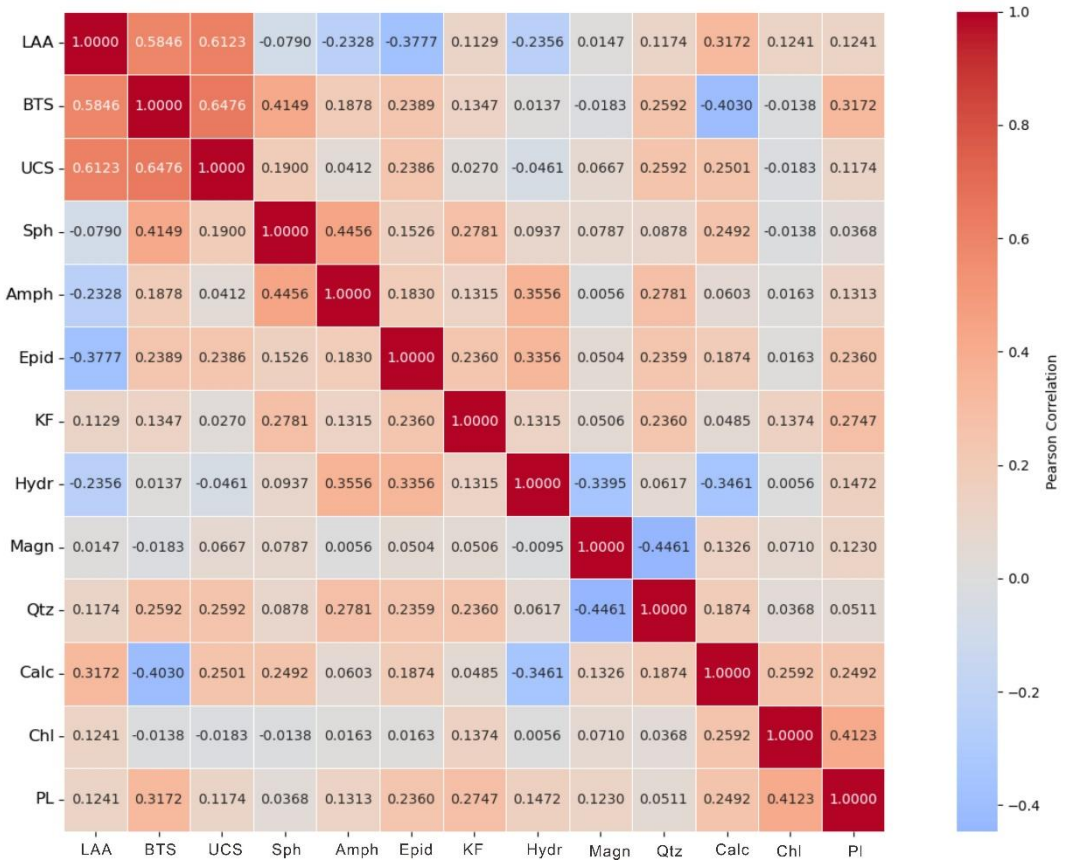

Fig. 5. *Heatmap of the correlation coefficients between variables*

3. Results and Discussion

3.1 Petrographic Analyses of Dolerites

The rocks of the Kirana hills have a fine to medium-grained texture categorized by hypidioblastic and sub-blastoporphyritic attributes. The plagioclase minerals present in the rocks range from andesine to labradorite. The plagioclase concentration varies between 20.4% and 30.5%, as shown in Figure 6. Amphibole is a secondary mineral found in rocks that plays a crucial role in their composition. It mainly arises as subidioblastic crystals (Petrounias *et al.*, 2018). The amphibole content varies between 0.5% and 10.8%. Chlorite is an essential mineral found in rocks, with a composition ranging from 20.7% to 52.5%. Pyribole undergoes alteration, resulting in the formation of a secondary mineral. Calcite can be found in rocks either as discrete grains or as aggregates. The production of this substance is mostly attributable to the modification of plagioclase. The calcite content varies between 4.5% and 19.2%. Quartz is categorized as an accessory mineral that is primarily discovered in the form of anhedral crystals. The composition varies between 2.2% and 4.5%.

Magnetite is a subordinate mineral that occurs as a crystal with an irregular shape. The composition ranges from 5.1% to 6.9%. The transformation of feldspar produces Hydromica and makes up approximately 2.0% to 2.5% of the rocks. Although it is a mineral that reacts, its quantity remains within a safe range. Orthoclase, a kind of K-feldspar, is classified as an accessory mineral. The substance transforms sericite and varies in composition from 3.1% to 4.5%. Epidotes are irregularly shaped crystals, and their composition ranges from 0.4% to 9.2%. Sphene is a widely distributed accessory mineral with a composition that varies from 0.5% to 2.0%. The quartz content in the dolerites ranges from 2.2% to 4.5%. These rocks are free from Alkali-Silica Reaction (ASR) Potential and can be used as aggregates in cement concrete that uses high alkali cement. The rock's hydrophilic mineral content, ranging from 2.2% to 4.5%, is within acceptable limits, making it appropriate for bitumen concrete. The sum of the detrimental substances in minerals varies from 2.0% to 2.5%, indicating that dolerites are safe and do not show any potential for Alkali-Silica Reaction (ASR).

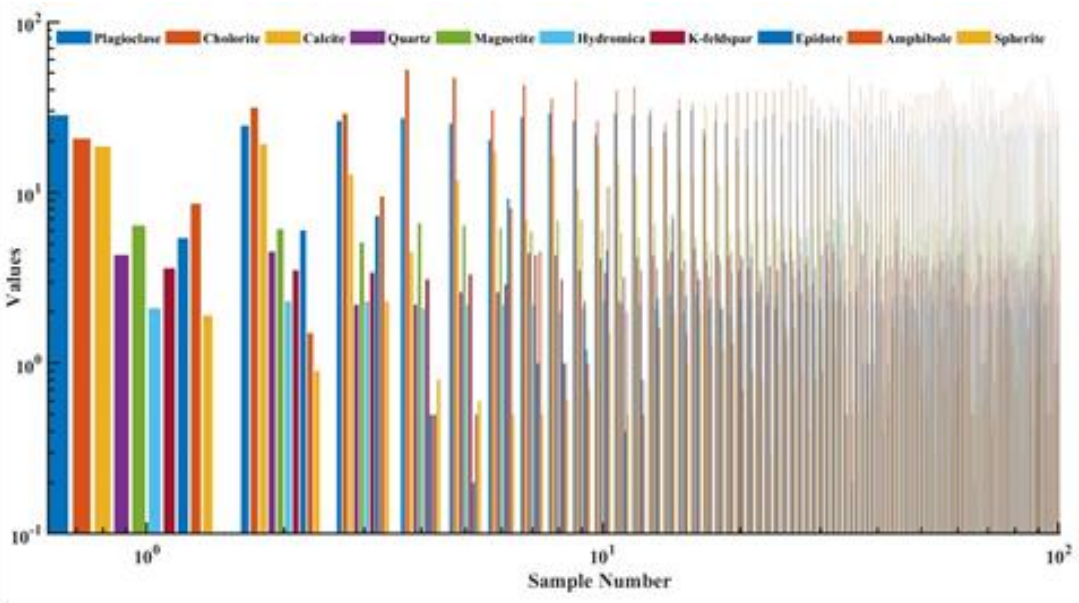

Fig. 6. *Petrographic Analyses of Dolerites, Kirana Hills, Pakistan*

3.2 Geotechnical Analyses

In the current research, each rock sample was subjected to the UCS test using prepared cores with a length-to-diameter ratio of 2:3. Figure 8 illustrates the average UCS values acquired for the rocks. The lowest recorded UCS value was 76.30 MPa, while the highest was 96.50 MPa.

In this research, experiments were performed on each Dolerite rock sample to ascertain its tensile strength. An absolute maximum of 9.1 MPa was measured for the BTS, with 6.1 MPa representing the minimum. The range of tensile strengths demonstrated by the Dolerite samples is denoted by these values, where a lower value corresponds to a reduced resistance to tension, and a higher value signifies an enhanced tensile strength (Naeem et al., 2019).

Aggregate strength and durability are assessed utilizing fundamental parameters, including LAA, Aggregate impact value (AIV), and aggregate crushing value (ACV) (Hussain et al., 2022). The Los Angeles abrasion values recorded in this research ranged from 9% to 15 %, as illustrated in Figure 7.

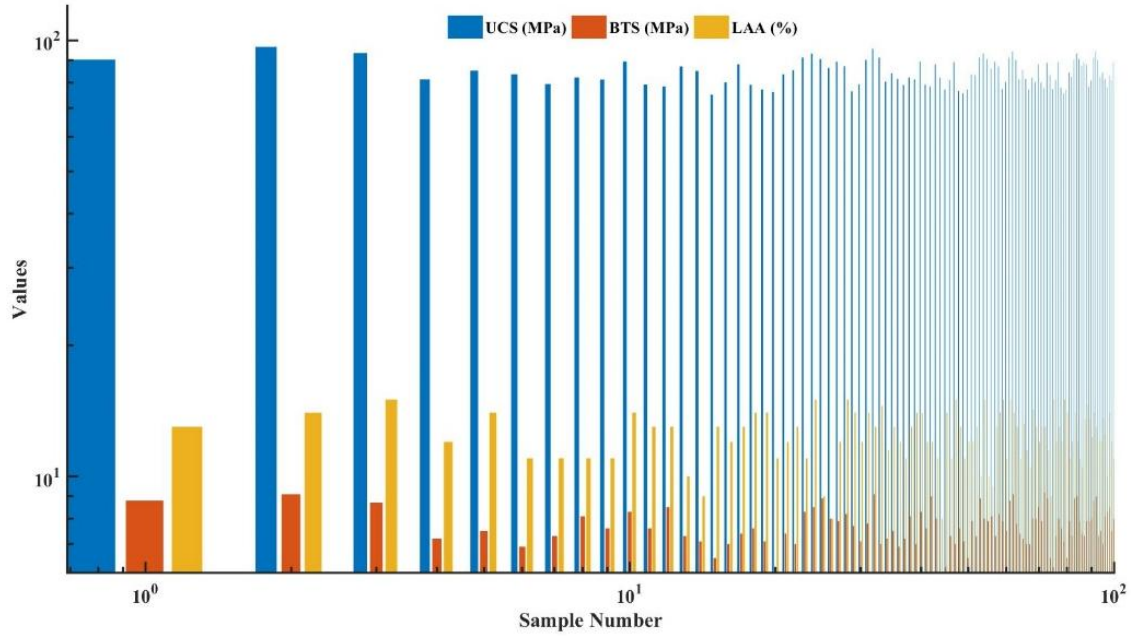

Fig 7. *Geotechnical Analyses of Dolerites, Kirana Hills, Pakistan*

3.3 ANN Approach

3.3.1 Levenberg–Marquardt (LM)

LM technique was used to estimate the mechanical properties of dolerites. The robustness and durability of these geological materials can be operated using fundamental metrics such as UCS, BTS, and LAA. The designed framework used in this research relies on organized data sets to predict the parameters. Figure 8 shows the training, validation, and testing model error histogram. The graph is inconsistent, as the bars converge on the red line in the centre. Moreover, RMSE was calculated by comparing the predicted and target values, as shown in Figure 9. RMSE data enhances and quantifies the adaptability and efficacy of the LM model compared to other evaluated models or approaches. The RMSE values shown in Figure 9 (a,b,c) vary from 0.8866 for UCS, 0.3023 for BTS, and 1.037 for LAA estimated outcomes. These data represent the difference between the expected and actual UCS, BTS, and LAA values. The findings indicate that the LM model is suitable for predicting the results of the UCS, BTS, and LAA.

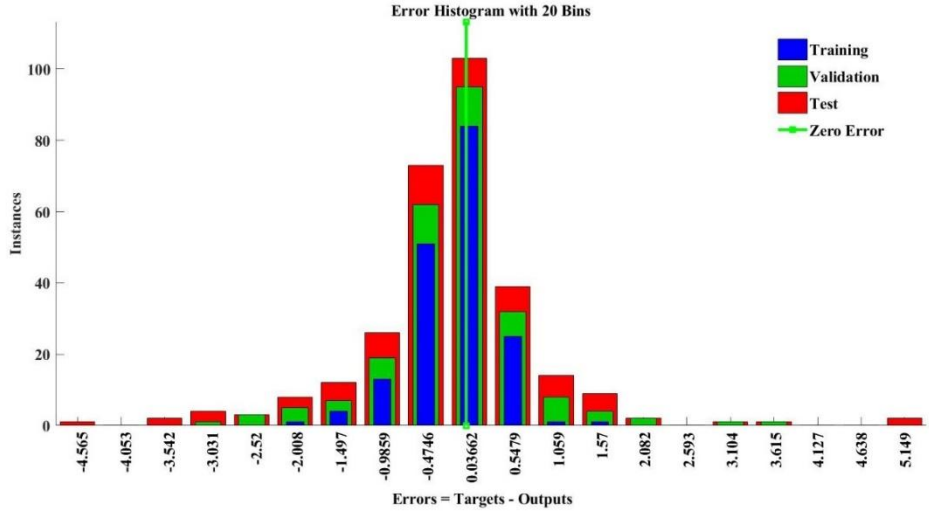

Fig. 8. *Error histogram of LM algorithm model.*

In addition, the precision values for each outcome range from 96% to 97%, which is a measurement of the model's prediction accuracy. This demonstrates that the LM model achieves high accuracy, as it constantly and accurately aligns its predictions with the experimental or target values.

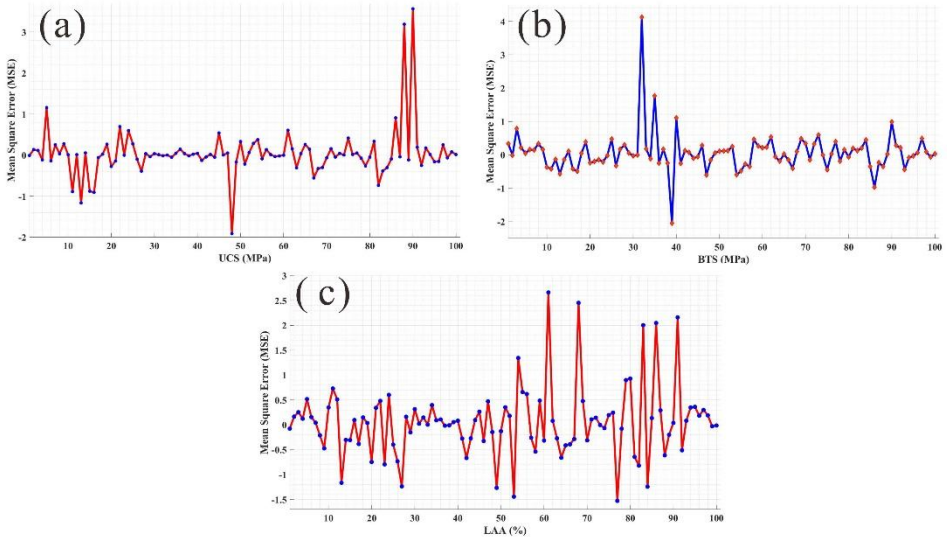

Fig. 9. *Graphs displaying the MSE of (a) UCS, (b) BTS, and (c) LAA based on LM analysis.*

Furthermore, Figure 11(a,b,c) displays the anticipated UCS, BTS, and LAA values associated with each data point in the dataset. This figure presents a thorough examination of the experimental results. The graphical

depiction demonstrates the high level of accuracy achieved by the LM model, with little absolute discrepancies in its predictions. The visual assessment in Figure 10 demonstrates the impressive ability of the LM model to accurately estimate UCS, BTS, and LAA measures, as seen by its alignment with the experimental data. This demonstrates the model's accuracy and competence in predicting these variables over the entire dataset.

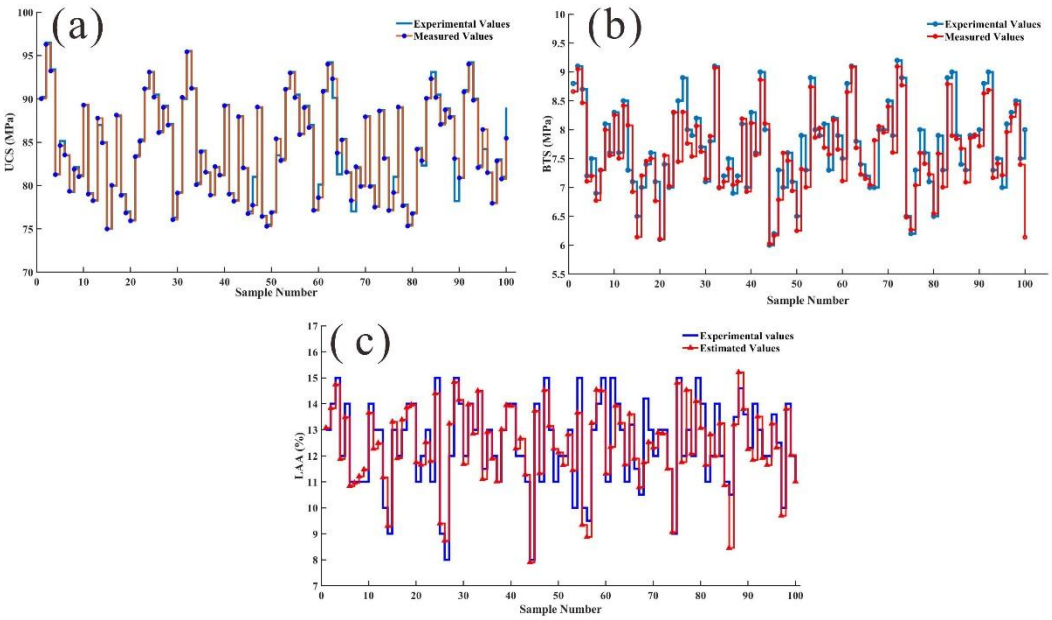

Fig. 10. *Variation between measured and predicted values of (a)UCS, (b)BTS, and (c)LAA based on LM*

Regression graphs have been generated to enhance the assertion of accuracy in demonstrating the relationship between the target or experimental data and the estimated values produced by the LM algorithm, as seen in Figure 11. Regression plots are crucial tools for visualization that comprehensively assess the level of consistency between the predicted values and the actual experimental data across several factors(Shah et al., 2022)..

Moreover, the correlations between the values of the mechanical characteristics predicted by LM and those seen in the experiment are displayed in Figure 11 (a). The lines obtained are well-fitted, and it is clear that the anticipated values of UCS, BTS, and LAA are, for the most part, close to the values obtained through the experiment. The R^2 value was recorded as 0.9994 between the experimental and estimated values of the mechanical strength of rocks. In conclusion, there are strong connections between the values of the predicted mechanical characteristics and those observed in the experiment.

In the residuals graph, most residuals cluster closely around the zero line, demonstrating a well-fitted model that, on average, precisely forecasts the mechanical strength based on petrographic parameters, as shown in Figure 11 (a). Generally, the high R^2 value of 0.9994 and the comprehensible pattern in the residual support the model's vigour and efficiency in describing the association between petrographic parameters and mechanical strength, as shown in Figure 11 (b).

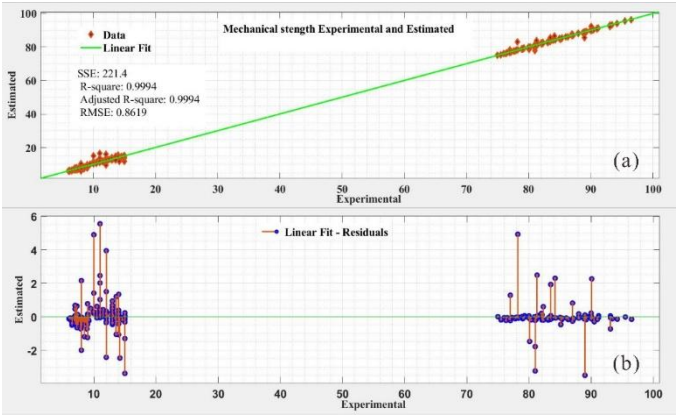

Fig. 11. *The graphs showing the (a) Relationship between experimental and estimated values of the rock mechanical properties and (b) residual graph based on LM*

The visual depictions of regression for several subsets of the data used for training, testing, and validation emphasize the model's ability to forecast accurately. The high regression value (R) of 0.9997 demonstrates a significant correlation between predicted and experimental results over the dataset, highlighting the model's reliable performance. The training set has a high regression value of 0.99998, demonstrating that the model fits the known data well. In the testing set, the regression value is slightly lower at 0.99893 but still substantial, signifying the model's ability to simplify fit to unknown data. Furthermore, the regression value of 0.99837 from the validation set proves the model's consistency and reliability. The plots exhibit high alignment between the points and the regression lines, indicating a strong relationship between the predicted and experimental values, confirming the model's efficacy. The separate regression plots for each outcome (UCS, BTS, and LLA) are shown in Figure 12(a,b,c,d).

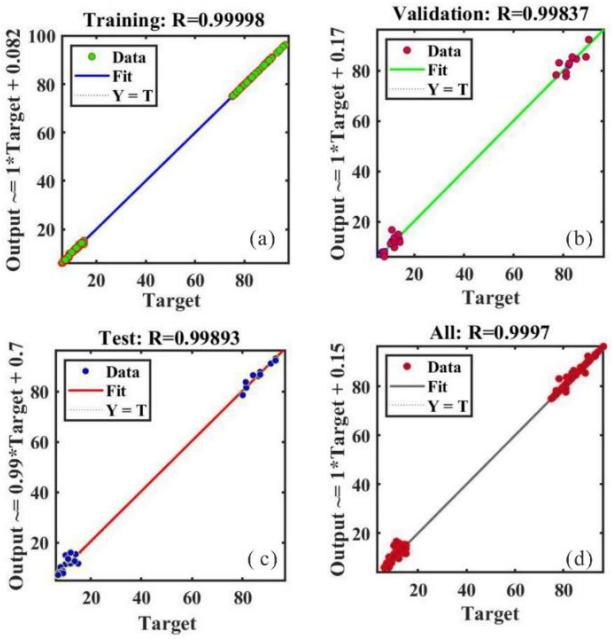

Fig. 12. *The prediction results of UCS, BTS, and LAA based on the LM model*

3.3.2 Bayesian regularization (BR)

The BR technique is used to train the model similarly to LM. Although the LM approach is faster, it often requires additional memory. BR may be more time-consuming but provide excellent generalization results for difficult, minor, or multifaceted datasets. The training terminates due to the use of adaptive weight reduction, also known as regularization.

The error histogram indicates that to mitigate overfitting, the model first exhibits a high MSE and then reduces its dependence on the training parameters. The graph illustrates that the model needs many epochs because of the little longer time required by BR. Figure 13 displays the model error histogram between training and testing. Based on the findings of this performance criteria, the model accurately forecasts the mechanical strength properties of the UCS, BTS, and LAA.

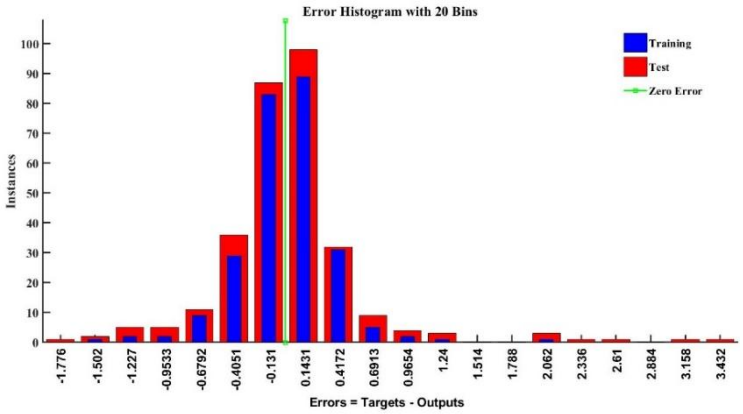

Fig. 13. *The error histogram based on the BR algorithm model.*

Furthermore, the RMSE was determined by comparing the projected values with the experimental values, as seen in Figure 14. The use of RMSE data enhances and quantifies the adaptability and efficacy of the LM model in comparison to other evaluated models or techniques. The RMSE values were recorded as 0.632 for UCS, as shown in Figure 14 (a), 0.2877 for BTS, as shown in Figure 14(b), and 0.4342 for the LAA, as shown in Figure 14 (c) predicted outcomes. The error level for UCS, BTS, and LAA between the predicted and actual values as shown by the values provided. These findings indicated that the BR model has high accuracy in forecasting the outcomes of the LAA, BTS, and UCS.

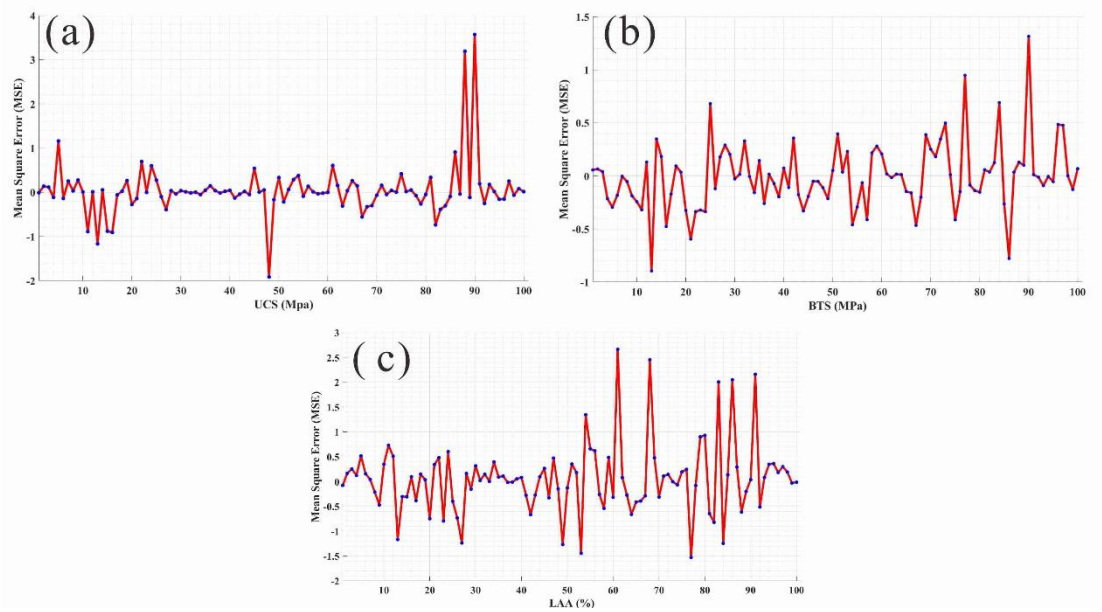

Fig. 14. *Root Mean Square Error (RMSE) of (A)UCS, (B)BTS, and (C)LAA based on BR*

The performance of the BR technique was evaluated by comparing experimental data with predictions made using ANN. The blue line on the y-axis shows the mechanical strength parameters' experimental values, whereas the red line represents projected values. Figure 15(a) exhibits the lines are nearly overlapped, indicating a high level of accuracy; however, in Figures 15(b) and 15 (c) for BTS and LAA, slight variations are observed, suggesting less accuracy compared to UCS. The graphical representation tremendously displays the exceptional accurateness obtained by the Baseline model, showcasing minimal absolute disparities in its predictions.

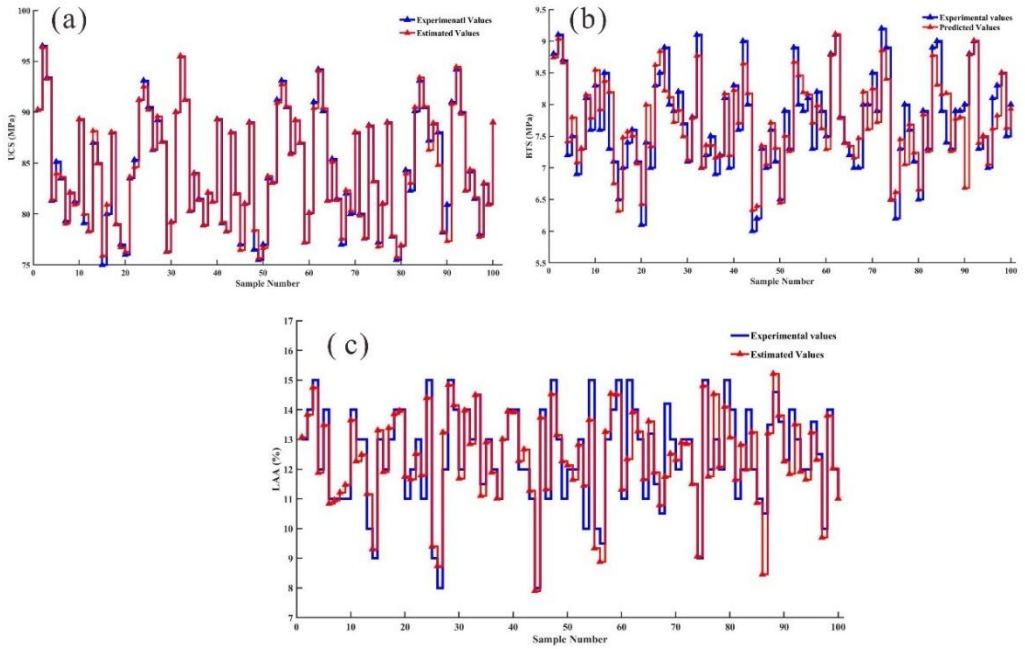

Fig. 15. *Graph showing the variation between measured and predicted values of (a)UCS, (b)BTS, and (c)LAA based on BR*

Moreover, Figures 16(a) and (b) display the correlations between the values of the mechanical characteristics predicted by BR and those seen in the experiment. The lines obtained are well-fitted, and the anticipated values of UCS, BTS, and LAA are, for the most part, equivalent to the values obtained through experimentation. In conclusion, there are strong connections between the values of the predicted mechanical characteristics and those observed in the experiment.

In addition, the residuals graph shows that most residuals cluster around the zero line, indicating a well-fitted model that accurately predicts mechanical strength from petrographic characteristics, as shown in Figure 16 (b). The model's high regression R^2 values of 0.9999 and the presence of a distinct residual pattern provide strong evidence for the model's validity and efficacy in defining petrographic features and mechanical strength. This model exhibits higher accuracy and value compared to the LM model, making it more reliable than the ML model.

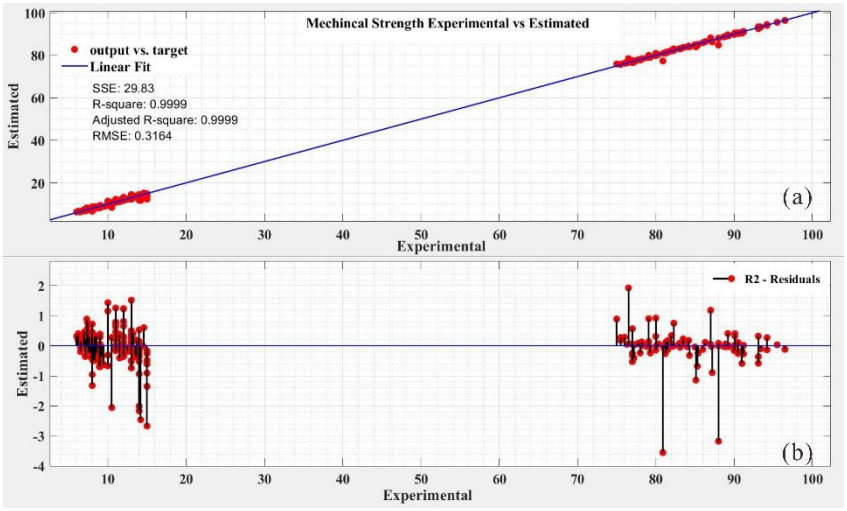

Fig. 16. *(a)Relationship between experimental and estimated values of the rock mechanical properties and (b) Residuals graph based on BR*

Subsequently, a regression analysis was conducted using the same methodology as the one employed for the LM model. Figure 17 (a,b,c) displays the training and testing correlations between the input and output variables of the model, providing an overview of the overall correlation. In each case, a linear fit with blue, green, and red colours is presented. The R-value of 0.99987 suggests that the model trained with Bayesian regularization accurately predicts the UCS, BTS, and LAA output.

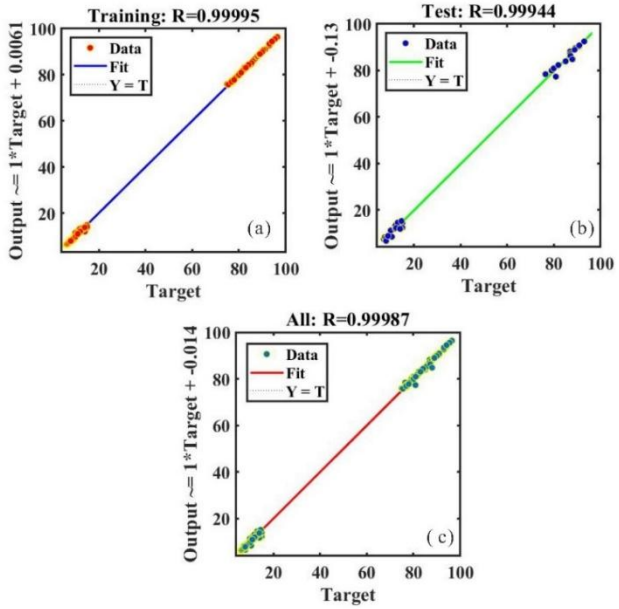

Fig. 17. *Regression analysis of BR between experimental and predicted mechanical strength of rock: (a) Training; (b) Testing; (c) Overall Dataset*

3.3.3 Scaled Conjugate Gradient (SCG)

The SCGB algorithm is employed to train the model. Figure 18 displays the histogram of model errors for training, validation, and testing. The graph illustrates the lack of convergence of the error bar bins towards the zero-error line. These findings indicate that the model exhibits much higher error values ranging from -8.768 to 7.924 compared to the LM and BR algorithms; it performs badly in predicting the mechanical strengths of rock.

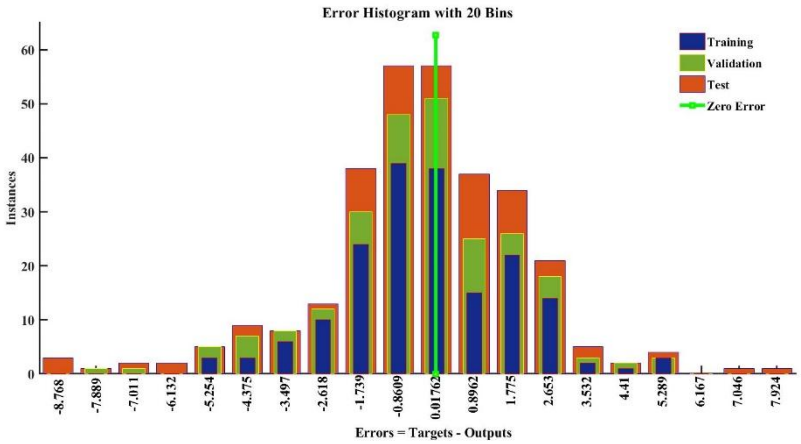

Fig. 18. *The error histogram based on SCG*

The RMSE values were recorded, which vary from 3.323 for UCS, as shown in Figure 19(a), 0.8912 for BTS, as shown in Figure 19(b), and 1.2432 for LAA, as shown in Figure 19 (c). These figures represent the degree of inaccuracy between the projected and actual values for UCS, BTS, and LAA. The results demonstrate that the SCG model is unsuitable for accurately forecasting the outcomes of the UCS, BTS, and LAA due to its high level of inaccuracy as compared to the LM and BR models.

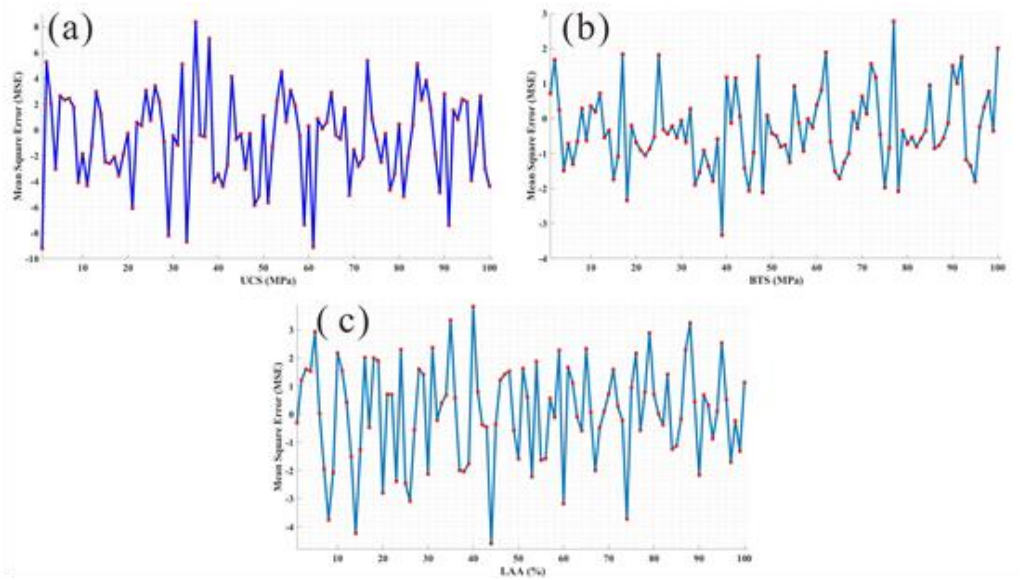

Fig. 19. *Root Mean Square Error (RMSE) of (A)UCS, (B)BTS and (C)LAA based on SCG*

Furthermore, a comprehensive analysis of the experimental and predicted findings of UCS, BTS, and LAA associated with each data point included in the SCG algorithm dataset was conducted, as presented in Figure 20. The graphical representation displays the accuracy obtained by the SCG model, showcasing maximum absolute disparities in its predictions. Through the visual examination in Figure 20 (a,b,c), the formidable capability of the SCG model to forecast UCS, BTS, and LAA metrics aligned with the experimental data is not reliable. These findings concluded that the SCG model is not well suited for predicting mechanical strength when compared to the LM and BR models

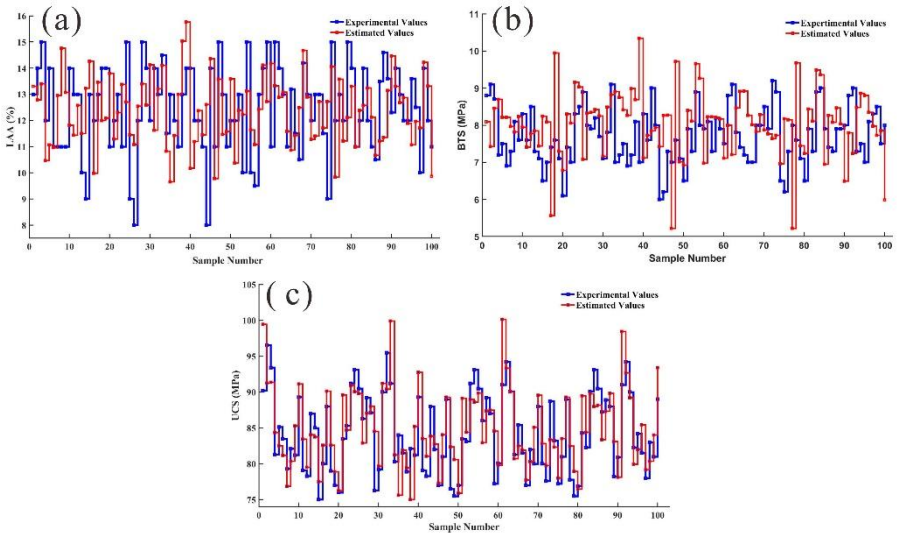

Fig. 20. *Graph showing the variation between measured and predicted values of (a)UCS, (b)BTS, and (c)LAA based on SCG*

The correlations between the values of the mechanical characteristics predicted by SCG and those seen in the experiment are presented in Figure 21. The results demonstrated that the predicted values of UCS, BTS, and LAA, for the most part, have illustrated more variability than the experimental values, as shown in Figure 21(a). The lines that were produced are not well-fitted. As a result, it can be stated that there are insufficient connections between the values of the predicted mechanical properties and those seen in the experiment, and the model has a minimal level of accuracy.

Moreover, the residuals graph demonstrates that most residual clusters are not located around the zero line, suggesting that the model is inappropriate and unsuitable for reliably predicting mechanical strength from petrographic features, as shown in Figure 21(b). In comparison to the LM and BR models, the SCG model has inadequate reliability, suggesting that it has far lower precision.

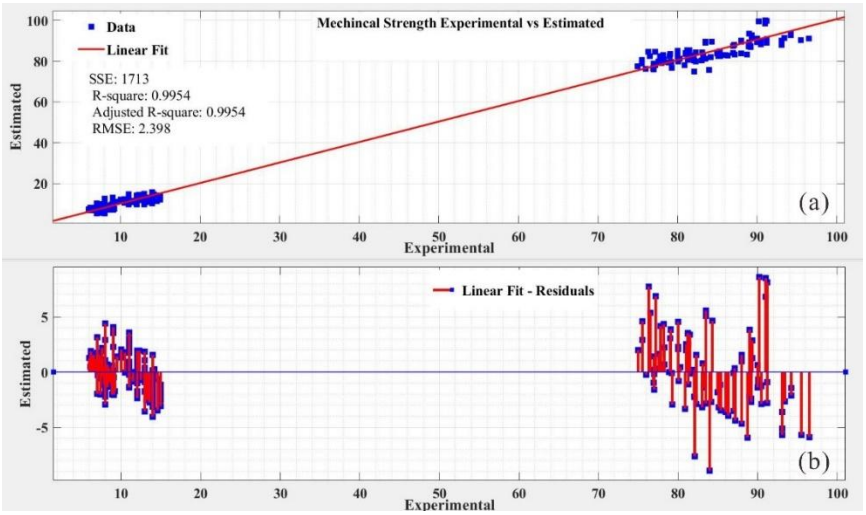

Fig. 21. *(a)Correlations between experimental and predicted values of the rock mechanical properties (b) Residual graphs based on SCG algorithm*

In addition, regression analyses were performed to illustrate the association between the input and output values of the model for training, validation, and testing. Figure 22(a,b,c) depicts the model's overall accuracy or relationship. Each instance displays a linear fit in a variety of colors. The R-value of 0.9972 reveals a poor or average model for predicting the mechanical strength of rock. The relationship between the variables is not linear. The regression analysis model demonstrates that the SCG algorithm is not well suited for predicting the mechanical strength of the rock when compared to the LM and BR models.

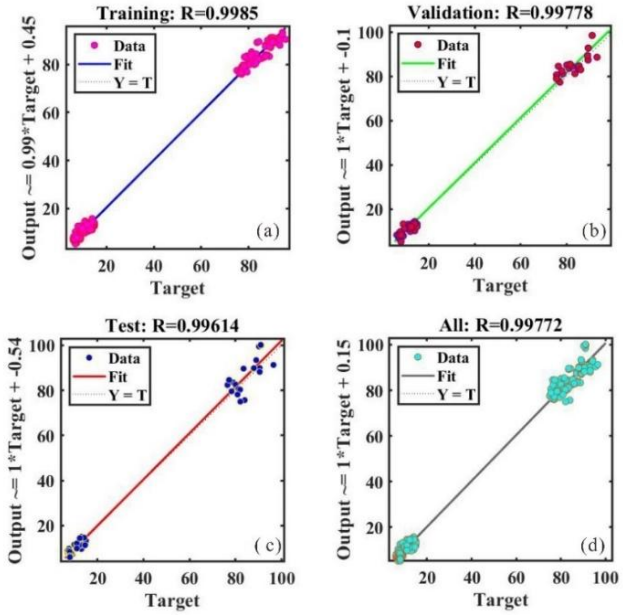

Fig. 22. *Regression analysis of SCG algorithm between experimental and predicted mechanical strength of rock: (a) Training; (b) Validation; (c) Testing; (d) Overall dataset.*

3.4 Taylor Diagrams

The Taylor diagrams are utilized (Khosravi *et al.*, 2021) to examine the training and testing outcomes of three models, as depicted in Fig. 23. Taylor diagrams integrate the correlation coefficient, RMSE, and standard deviation into a single polar diagram based on their cosine relationship. In addition, the reference point accurately represents the UCS, BTS, and LAA, whereas points closer to the referenced show lower-centered RMSE values and higher model capabilities. During the training and testing stages, BR demonstrates superior performance compared to LM, while SCG performs the least effectively, as shown in Figure 23.

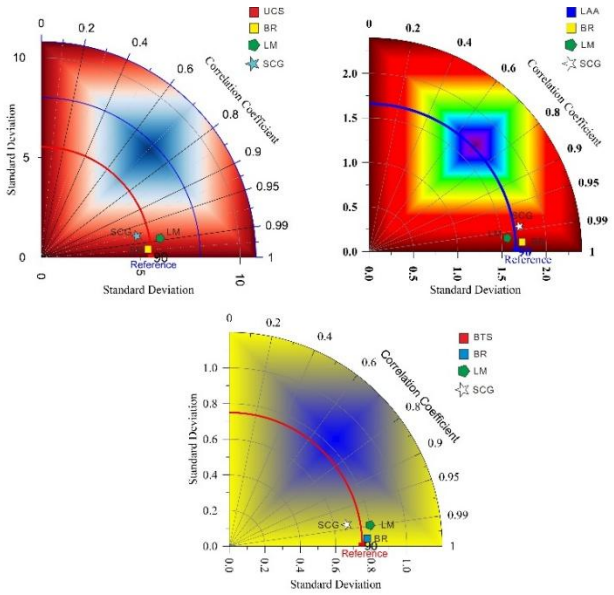

Fig. 23. *The Taylor diagrams of the UCS, BTS, and LAA based on LM, BR, and SCG*

3.5 Comparison of BR, LM, and SCG Models

In the assessment of three different approaches using both experimental data and ANN predictions, the performance of the models was carefully evaluated. Figure 24 (a) associates the experimentally observed values of UCS with those estimated by the different algorithms. Remarkably, the predictions from the BR and LM algorithms demonstrate high accuracy, with their lines nearly flawlessly overlapping. In contrast, the predictions resulting from the SCG algorithm show more noticeable deviations, demonstrating less precision in predicting UCS. The BTS assessment, shown in Figure 24 (b), reveals that both the BR and LM models consistently outperform the SCG algorithm in predictive accuracy. The graphical representation further emphasizes the strong performance of BR and LM, highlighting the significant discrepancies observed in the SCG model's predictions. Similarly, the predictions for LAA, as shown in Figure 24 (c), indicate a higher accuracy for the BR model, followed closely by the LM model, while the SCG algorithm again demonstrates comparatively poorer performance. This comparative analysis underscores the BR model's superior accuracy across various parameters when compared to the LM and SCG models.

Beyond the accuracy of predictions, computational efficiency plays a crucial role in the selection of the most suitable model for practical applications. The BR algorithm, while demonstrating exceptional accuracy, tends to require longer processing times and more memory usage due to its complex network structure and iterative optimization process. The LM algorithm, on the other hand, achieves similar predictive accuracy as the BR model but with significantly faster processing times and lower memory requirements, making it more suitable for time-sensitive applications and scenarios with limited computational resources.

In contrast, the SCG algorithm, although computationally more efficient in terms of processing time, lags in terms of accuracy. The computational speed of SCG may make it an attractive choice for applications where speed is more critical than high precision. However, in practical applications where predictive accuracy is paramount, such as in geotechnical engineering or geological exploration, the BR and LM models are more appropriate despite their higher computational cost. Therefore, the choice of algorithm should be guided not only by the desired accuracy but also by the available computational resources and the specific needs of the application, balancing between accuracy, processing time, and memory usage.

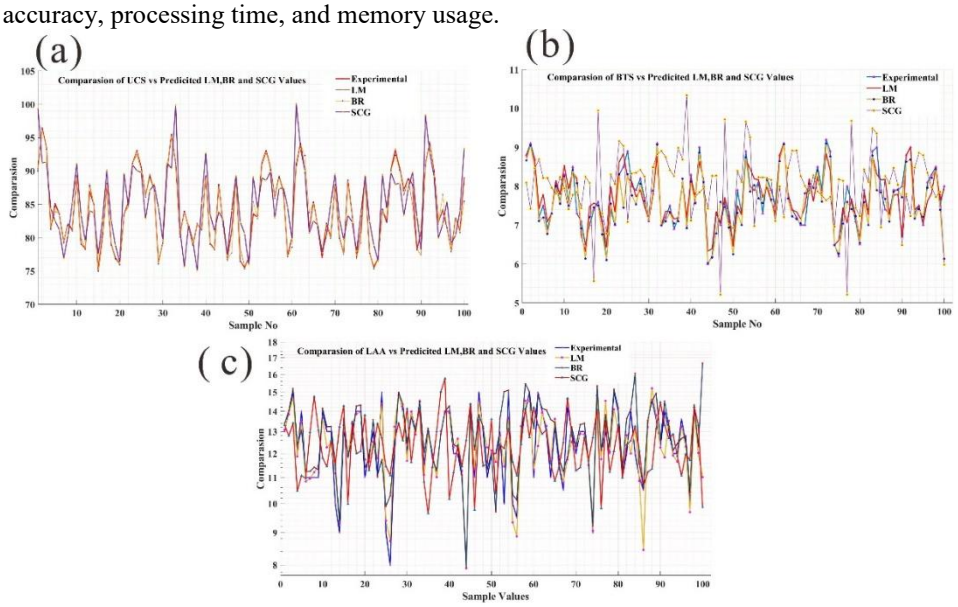

Fig. 24. *Comparison of mechanical strength parameters vs predicted values of (a) LM, (b)BR, and (c)SCG*

3.6 Sensitivity Analyses

Sensitivity analysis evaluates how individual input variables influence the output variables, providing insight into the impact of each mineral component on the rock's mechanical strength. The results highlight that the influence of input variables on the output parameters increases with higher sensitivity levels. Previous studies, such as those by Shang et al., have shown that certain input variables significantly affect the prediction of output variables (Ji *et al.*, 2017).

In this research, a sensitivity analysis was conducted to assess the influence of individual mineral components, Plagioclase, chlorite, calcite, quartz, magnetite, Hydromica, K-feldspar, epidote, amphibole, and spherite on the rock's UCS, BTS, and LAA. The analysis results, shown in Figure 25, indicate that Plagioclase and chlorite are the most influential variables affecting the mechanical strength of the rock. This aligns with findings from (Pan *et*

al., 2016), who emphasized that Plagioclase and chlorite are crucial for the compressive strength of rocks. However, while Plagioclase and chlorite are the primary contributors to the rock's mechanical properties, the analysis also revealed that other minerals, such as calcite, quartz, magnetite, Hydromica, K-feldspar, epidote, amphibole, and spherite, have a more limited impact. Notably, minerals like quartz, spherite, and Hydromica were identified as the least significant contributors to the variability of UCS, BTS, and LAA, with sensitivity scores of 0.0483, 0.0484, and 0.0474, respectively.

This insight into the relative significance of various minerals suggests that while minerals such as Plagioclase and chlorite should be prioritized in predicting rock strength, the influence of minerals with lower significance (such as quartz and Hydromica) may be negligible in the context of the mechanical strength parameters studied. These findings underscore the importance of focusing on key mineralogical factors when developing predictive models for rock mechanical properties.

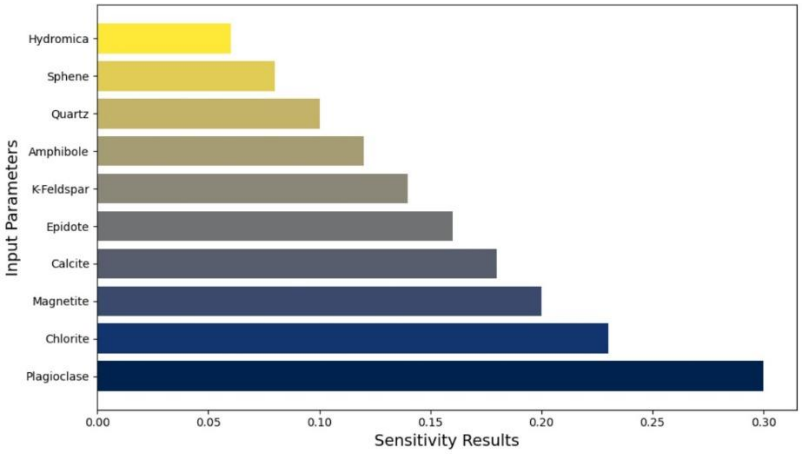

Fig. 25. *Variable importance of input parameters to mechanical strength parameters (US, BTS, LAA)*

3.7 Model Validation

Twenty rock samples were prepared into standard specimens and tested for mineralogical, UCS, UCS, BTS, and LAA to ensure the BR Model's applicability. The developed BR model employed petrographic parameters as input and produced mechanical strength as output. The R^2 and MSE were calculated using the BR model, as seen in Figure 26(a,b,c,d). In addition, the anticipated and observed values of UCS, BTS, and LAA are compared. When the developed BR model is used for the new datasets from the validation data, it obtains an R^2 of 0.99 and an MSE ranging from -3.60 to 3.88, as seen in Figure 26(a,b,c,e). The measured ratios of UCS, BTS, and LAA to the anticipated values are greater than the actual values. The findings acquired demonstrate the significant technical applicability of the proposed approach. The model suggested in this research can accurately estimate the UCS, BTS, and LAA of rock samples to an adequate level.

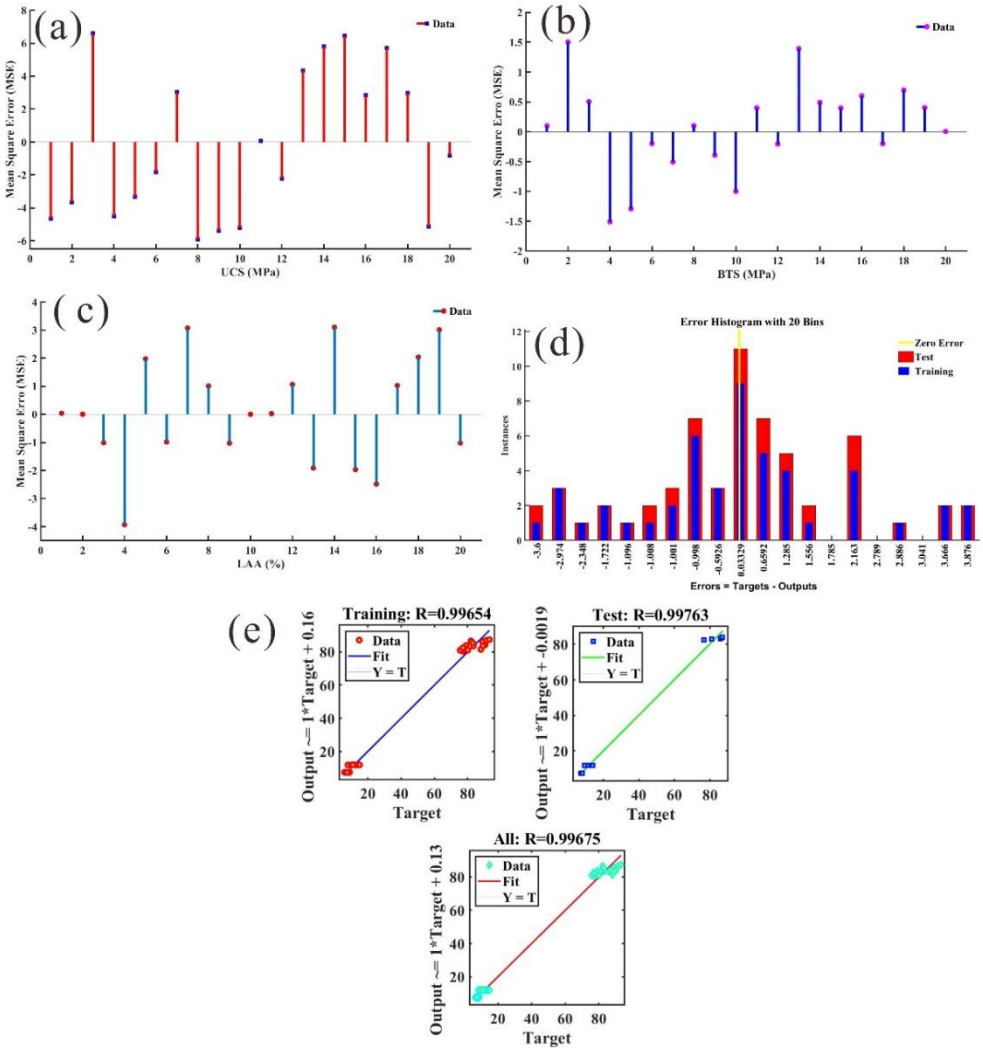

Fig. 26. *The predicted results of 20 validation datasets*

4 Conclusion

This research conducted 100 laboratory tests on rock samples from the Kirana Hills to develop an advanced predictive model for important rock strength parameters, namely UCS, BTS, and LAA. The study underscores the crucial role of artificial neural networks (ANNs) as a powerful tool for accurate predictions, particularly when traditional empirical correlations fall short. Mineralogical data was utilized as the input for constructing the predictive model, with rock strength characteristics serving as the output. Through this approach, the research successfully established predictive models using the LM, BR, and SCG algorithms.

The performance of the three algorithms was rigorously evaluated, with the LM, BR, and SCG methods achieving accuracy rates of 99%, 98%, and 95%, respectively. The corresponding root mean square error (RMSE) values for these models were 0.8619, 0.3164, and 2.398, indicating the varying levels of their effectiveness. The SCG algorithm, however, proved to be the least effective, showing poor correlation and high RMSE values compared to the other models, which made it unsuitable for accurately predicting the mechanical strength of rocks. In contrast, the BR model outperformed both the LM and SCG models, achieving an outstanding R-value of 99.99% and the lowest RMSE of 0.3164. While the LM model achieved a very similar R-value of 99.97%, it was significantly faster in terms of processing time compared to the BR algorithm. These results demonstrate that both the LM and BR algorithms are highly effective models for predicting the mechanical strength parameters of rocks, including UCS, BTS, and LAA. Sensitivity analysis further identified Plagioclase and Chlorite as the primary variables influencing the mechanical strength of rocks, while other variables had a comparatively lesser impact on the predictions. This highlights the importance of focusing on key mineralogical components to improve model accuracy.

In conclusion, the LM and BR algorithms demonstrated exceptional accuracy, offering a dual advantage of both time and cost efficiency in estimating the mechanical properties of rocks. These models represent a significant advancement in geological and engineering investigations, providing a reliable, cost-effective tool for rock property analysis. Their integration into geological studies can streamline decision-making processes, enabling more informed choices in the exploration, mining, and engineering sectors. However, the research also suggests that future studies should expand the model's scope by including a broader range of rock types and incorporating a larger dataset, which will likely improve the overall performance and robustness of the predictive models. Additionally, extending the model to include other important rock properties, such as Young's modulus, would further enhance its applicability and utility, making it even more valuable for comprehensive geological and engineering analyses.

References

Alber, M. and Kahraman, S. (2009) 'Predicting the uniaxial compressive strength and elastic modulus of a fault breccia from texture coefficient', Rock Mechanics and Rock Engineering, 42(1), p. 117. DOI 10.1007/s00603-008-0167-x

ASTM, A.S.A. (2008) 'C131', C131M: Standard Test Method for Resistance to Degradation of Small-Size Coarse Aggregate by Abrasion and Impact in the Los Angeles Machine. ed. https://store.astm.org/c0131_c0131m-20.html

Bandini, A. and Berry, P. (2013) 'Influence of marble's texture on its mechanical behavior', Rock mechanics and rock engineering, 46, pp. 785–799.DOI 10.1007/s00603-012-0315-1

Borgonovo, E. and Plischke, E. (2016) 'Sensitivity analysis: A review of recent advances', European Journal of Operational Research, 248(3), pp. 869–887.https://doi.org/10.1016/j.ejor.2015.06.032

C170/C170M-17, A. (2017) 'Standard Test Method for Compressive Strength of Dimension Stone', ASTM International [Preprint]. West Conshohocken, PA, 19428, USA.https://store.astm.org/c0170_c0170m-17.html

Culshaw, M.G. (2015) ‘Ulusay, R (ed.), 2015. The ISRM suggested methods for rock characterization, testing and monitoring: 2007–2014: Cham, Switzerland: Springer. DOI 10.1007/978-3-319-007713-0', Bulletin of Engineering Geology and the Environment, 74(4), pp. 1499–1500.

Deere, D.U. and Miller, R.P. (1966) Engineering classification and index properties for intact rock. Illinois Univ At Urbana Dept Of Civil Engineering.https://trid.trb.org/View/119043

Dogan, A.U. et al. (2006) 'Classifications of hardgrounds based upon their strength properties', Carbonates and Evaporites, 21, pp. 14–20.https://link.springer.com/article/10.1007/BF03175464

Hemmati, A. et al. (2020) 'The effect of mineralogy and textural characteristics on the strength of crystalline igneous rocks using image-based textural quantification', Engineering Geology, 266, p. 105467.https://doi.org/10.1016/j.enggeo.2019.105467

Hussain, J. et al. (2022) 'Aggregate Suitability Assessment of Wargal Limestone for Pavement Construction in Pakistan', Open Journal of Civil Engineering, 12(01), pp. 56–74. Available at: https://doi.org/10.4236/ojce.2022.121005.

Hussain, J. et al. (2025) 'Geospatial mapping of potential aggregate resources using integrated GIS-AHP, geotechnical, petrographic and machine learning approaches', Earth Science Informatics, 18(4), p. 336.https://doi.org/10.1007/s12145-025-01794-0

Hussain, Javid et al. (2023) 'Suitability Assessment Constraints of Potential Aggregate Resources Using an Integrated GIS Approach', Journal of Materials in Civil Engineering, 35(9), p. 4023307.https://doi.org/10.1061/JMCEE7.MTENG-1468

Hussain, Javid et al. (2024) 'Petrological controls on the engineering properties of carbonate aggregates through a machine learning approach', Scientific Reports, 14(1), p. 31948.https://doi.org/10.1038/s41598-024-83476-3

Jahed Armaghani, D. et al. (2016) 'Application of several non-linear prediction tools for estimating uniaxial compressive strength of granitic rocks and comparison of their performances', Engineering with Computers, 32, pp. 189–206.DOI 10.1007/s00366-015-0410-5

Ji, X. et al. (2017) 'Prediction of dissolved oxygen concentration in hypoxic river systems using support vector machine: a case study of Wen-Rui Tang River, China', Environmental Science and Pollution Research, 24, pp. 16062–16076.DOI 10.1007/s11356-017-9243-7

Kamani, M. and Ajalloeian, R. (2019) 'Evaluation of engineering properties of some carbonate rocks trough corrected texture coefficient', Geotechnical and Geological Engineering, 37, pp. 599–614.https://doi.org/10.1007/s10706-018-0630-8

Khajevand, R. and Fereidooni, D. (2018) 'Assessing the empirical correlations between engineering properties and P wave velocity of some sedimentary rock samples from Damghan, northern Iran', Arabian Journal of Geosciences, 11, pp. 1–17.https://doi.org/10.1007/s12517-018-3810-1

Khan, M.W. et al. (2017) 'Petrographic and Geochemical Analyses of Kirana Hills Shield Rocks around Sargodha and Economic Potential', International Journal of Economic and Environmental Geology, 8(2), pp. 9–20.https://www.econ-environ-geol.org/index.php/ojs

Khan, N.A. et al. (2021) 'Numerical analysis of electrohydrodynamic flow in a circular cylindrical conduit by using neuro evolutionary technique', Energies, 14(22), p. 7774.https://doi.org/10.3390/en14227774

Khan, N.A. et al. (2022) 'Investigation of Non-linear Vibrational Analysis of Circular Sector Oscillator by Using Cascade Learning', Advances in Materials Science and Engineering, 2022. https://doi.org/10.1155/2022/1898124

Khosravi, K. et al. (2021) 'Short-term River streamflow modeling using Ensemble-based additive learner approach', Journal of Hydro-environment Research, 39, pp. 81–91.https://doi.org/10.1016/j.jher.2021.07.003

López, C. (2023) 'Artificial intelligence and advanced materials', Advanced Materials, 35(23), p. 2208683,DOI: 10.1002/adma.202208683 .

Manouchehrian, A., Sharifzadeh, M. and Moghadam, R.H. (2012) 'Application of artificial neural networks and multivariate statistics to estimate UCS using textural characteristics', International Journal of Mining Science and Technology, 22(2), pp. 229–236.https://doi.org/10.1016/j.ijmst.2011.08.013

Momeni, E. et al. (2015) 'Prediction of unconfined compressive strength of rocks: a review paper', Jurnal Teknologi, 77(11).DOI: https://doi.org/10.11113/jt.v77.6393

Naeem, M. et al. (2019) 'Physical characterization and alkali carbonate reactivity (ACR) potential of the rocks from Bauhti Pind and Bajar area Hassan Abdal, Pakistan', SN Applied Sciences, 1(7), pp. 1–9. Available at: https://doi.org/10.1007/s42452-019-0736-5.https://doi.org/10.1007/s42452-019-0736-5

Ozcelik, Y., Bayram, F. and Yasitli, N.E. (2013) 'Prediction of engineering properties of rocks from microscopic data', Arabian Journal of Geosciences, 6, pp. 3651–3668.DOI 10.1007/s12517-012-0625-3

Pan, R. et al. (2016) 'Influence of mineral compositions of rocks on mechanical properties', in ARMA US Rock Mechanics/Geomechanics Symposium. ARMA, p. ARMA-2016.

Petrounias, P. et al. (2018) 'The effect of petrographic characteristics and physico-mechanical properties of aggregates on the quality of concrete', Minerals, 8(12), p. 577.https://doi.org/10.3390/min8120577

Pianosi, F. et al. (2016) 'Sensitivity analysis of environmental models: A systematic review with practical workflow', Environmental modelling & software, 79, pp. 214–232.https://doi.org/10.1016/j.envsoft.2016.02.008

Shah, S.Y.A. et al. (2022) 'Physio-Mechanical Properties and Petrographic Analysis of NikanaiGhar Limestone KPK, Pakistan', Open Journal of Civil Engineering, 12(02), pp. 169–188. Available at: https://doi.org/10.4236/ojce.2022.122011.DOI: 10.4236/ojce.2022.122011

Stroisz, A.M. et al. (2025) 'Laboratory Approach for Characterizing Degraded Shale Material', Rock Mechanics and Rock Engineering, pp. 1–20.https://doi.org/10.1007/s00603-025-04558-w

Ugur, I., Demirdag, S. and Yavuz, H. (2010) 'Effect of rock properties on the Los Angeles abrasion and impact test characteristics of the aggregates', Materials Characterization, 61(1), pp. 90–96. Available at: https://doi.org/10.1016/j.matchar.2009.10.014.https://doi.org/10.1016/j.matchar.2009.10.014

Woodland, S.K. et al. (2023) 'Paint Speckle Application Recommendations for Digital Image Correlation Analysis of Brazilian Tensile Strength Tests on Low-Porosity Rocks', Rock Mechanics and Rock Engineering, pp. 1–13.https://doi.org/10.1007/s00603-023-03604-9

Yagiz, S. (2011) 'P-wave velocity test for assessment of geotechnical properties of some rock materials', Bulletin of Materials Science, 34, pp. 947–953.https://link.springer.com/article/10.1007/s12034-011-0220-3